

NACA TN 3614

7066

56-3-23

# NATIONAL ADVISORY COMMITTEE FOR AERONAUTICS

TECHNICAL NOTE 3614

FLOW STUDIES ON DROOPED-LEADING-EDGE  
DELTA WINGS AT SUPERSONIC SPEED

By William H. Michael, Jr.

Langley Aeronautical Laboratory  
Langley Field, Va.



Washington  
January 1956

AFMDC

TECHNICAL LIBRARY





0066441

TECHNICAL NOTE 3614

## FLOW STUDIES ON DROOPED-LEADING-EDGE

## DELTA WINGS AT SUPERSONIC SPEED

By William H. Michael, Jr.

## SUMMARY

An experimental investigation has been made to study the flow over delta wings with drooped leading edges. Vapor-screen, pressure-distribution, and ink-flow tests were made on a series of semispan delta wings with semiapex angles of  $15^\circ$ ,  $22.5^\circ$ , and  $31.75^\circ$  and with 10 percent and 20 percent of the semispans drooped  $15^\circ$  in streamwise sections. The tests were made at a Mach number of 1.9.

The tests indicated that flow separation occurred on all the wings in the series tested. The separated regions on the wings with 10 and 20 percent of the semispans drooped were similar to one another. Integrated pressure distributions showed that, for equal angles of attack, the loadings on the wings with 20 percent of the semispans drooped were less than those on the wings with 10 percent of the semispans drooped.

In a general comparison with undrooped delta wings, the drooped-leading-edge wings showed no particular advantage from a standpoint of preventing separation. The drooped-leading-edge wings had a disadvantage in loading, the loading in some cases being considerably less than that on the corresponding undrooped wings.

## INTRODUCTION

A recent study has been made to investigate some aspects of the physical nature of the flow over a series of flat-plate delta wings. The results of the study (presented in ref. 1) give some qualitative information pertaining to flow separation on flat wings.

In the present study, an investigation has been made to study flow phenomena on delta wings with drooped leading edges. Wings with drooped or cambered leading edges can have stability and lifting characteristics which are desirable at subsonic speeds. At supersonic speeds these desirable characteristics of drooped leading edges may no longer be

present. The purpose of the present investigation is to determine in a qualitative manner the effects of leading-edge droop on the flow separation and loading characteristics of delta wings at supersonic speed.

### SYMBOLS

$\alpha$	angle of attack, deg
$\epsilon$	wing semiapex angle, deg
$b/2$	wing semispan, in.
$M$	Mach number
$\frac{\Delta p}{q}$	pressure coefficient, $\frac{p_z - p}{q}$
$p_z$	local static pressure
$p$	free-stream static pressure
$q$	free-stream dynamic pressure
$\mu$	Mach angle, $\sin^{-1} \frac{1}{M}$
$y$	spanwise coordinate, in.

### APPARATUS AND MODELS

#### Blowdown Jet

The tests for this investigation were made in a 9- by 6-inch Mach number 1.9 blowdown jet of the Langley gas dynamics laboratory. The test section was equipped with a boundary-layer scoop-off plate to minimize the effect of boundary layer on the semispan models. (See fig. 1.) With this boundary-layer scoop-off plate, the maximum boundary-layer thickness was calculated to be about 1 percent of the span for the wing with the smallest span. The present tests were made at a Reynolds number of  $1.58 \times 10^6$  per inch.

### Flow-Visualization Apparatus

A vapor-screen technique similar to that used in reference 2 was used in the present tests to observe the flow phenomena around delta wings. In this technique, water was inserted in the air-supply line upstream of the settling chamber. After the water was broken into very small droplets by the settling-chamber turbulence screens and expanded through the nozzle, it appeared in the test section as a fog. A mercury-vapor light source was used to produce a narrow slit of intense light perpendicular to the tunnel axis. (See fig. 2.) The light scattered by the particles appeared as a screen of illumination on which changes of density showed up as changes in intensity of illumination; therefore, regions of concentrated vorticity and shock waves could be observed. An aerial camera was used to take photographs of the vapor screen. The change in Mach number with the addition of water was found by static-pressure measurements to be small ( $\Delta M = -0.03$ ) with respect to the Mach number obtained without water addition.

### Models

The leading edges of the semispan delta-wing models used in this investigation were drooped by bending them about a ray through the apex. When the wings were viewed in streamwise sections, the drooped portions of the wings made an angle of approximately  $15^\circ$  with respect to the undrooped portions. Wings with 10 percent and 20 percent of the semispan drooped and with semiapex angles of  $15^\circ$ ,  $22.5^\circ$ , and  $31.75^\circ$  were used. Drawings of the models are given in figure 3, where the dimensions of the models before drooping the leading edges are shown in the left column. In order to facilitate construction of the models, the leading edges were not made extremely sharp as for the models of reference 1, but were given a small radius of the order of 1 percent of the wing semispan. The maximum thickness ratio of the wings was constant for a given wing and was approximately 3 to 5 percent.

Pressure orifices were installed first on one surface of the model and then on the other to give pressure distributions on both surfaces. The pressure orifices on the upper surface of the wings were used to insert ink onto the wing surface for the ink-flow studies, which were made only for the wings with 10 percent of the semispans drooped. The parts of the wings to the rear of the pressure orifices were painted white to make the ink pattern more easily visible; however, for some angles of attack the reflection of the light from the wing surface caused some interference with the ink-flow observations.

## TESTS AND RESULTS

Vapor-screen tests were made at one chordwise position for each of the wing models for angles of attack of  $0^\circ$  to  $20^\circ$ , and the vapor-screen photographs are presented in figures 4 to 9. The flow observed over the wing appeared to be steady. These photographs were taken from a position outside the tunnel and at an angle with the tunnel axis; thus, the separated regions do not appear in the photographs at their true distances above the wing surface, although the spanwise positions are correctly represented. The actual distances of the separated regions above the wing surface can be obtained from the camera angle and the wing angle of attack. For these photographs, the actual distances above the wing surface are of the order of twice the observed distances because the camera angle is approximately  $60^\circ$  relative to the tunnel center line.

Pressure distributions were measured normal to the surface on the upper and lower surfaces of each of the wing models, and these results are presented in figures 10 to 15. Orifices were installed and tests made separately on the upper and lower surfaces. In order to give a comparison of the corresponding loadings on the wings, the pressure distributions were integrated and the results are presented in figures 16 to 18 along with the results for the flat undrooped wings of reference 1. For these comparisons, the components of the loadings normal to the undrooped portion of the wings were used in the integrations.

Ink-flow test results on the wings with 10 percent of the semispans drooped are presented in the photographs of figures 19 to 21.

### DISCUSSION

The vapor-screen photographs are essentially self-explanatory, but some of the more important aspects of the photographs should be noted. The dark regions in the photographs correspond to regions of low density; hence, they show less reflection from the particles in the airstream than do the surrounding regions. (See ref. 1.) In various photographs the dark regions may indicate concentrated vortex cores, regions of separated flow, or low-density regions preceding shock waves.

The primary interest in the pressure distributions for the present study centers on the conditions on the suction or upper surfaces of the wings and on the integrated loadings. Ink-flow studies were included to give an indication of the flow characteristics in the boundary layer.

Wings With Semiapex Angles of  $15^\circ$

Flow separation, as indicated by separated regions of vorticity, is first observed at an angle of attack of  $12^\circ$  on the wings with 10 and 20 percent of the semispans drooped. (See figs. 4 and 5.) The regions of separation move inboard and increase in size with increase in angle of attack. Increasing the amount of droop from 10 to 20 percent semispan appears to have little effect on the size or location of the separated regions, except that on the wing with 20 percent of the semispan drooped there is some indication of an additional flat region of separation near the leading edge at the higher angles of attack.

The upper-surface pressure distributions in figures 10 and 11 show that, for the higher angles of attack, large negative pressures are obtained over the outboard 50 or 60 percent of the semispan. The inboard extents of these negative pressure regions correspond approximately to the inboard extents of the observed separated regions of vorticity. At low angles of attack and near the leading edges, pronounced effects of leading-edge droop on the pressure distributions are observed. The integrated pressure distributions in figure 16 show that there is little difference in the total loadings on the wings with 10 and 20 percent of the semispans drooped.

The ink-flow tests, which were made only for the wing with 10 percent of the semispan drooped (fig. 19), indicate that there is probably no flow separation at the leading edge for angles of attack of  $8^\circ$  and less. If it is assumed that the flow over the wing is conical and, thus, that the pressure distributions at all chordwise positions are like those in figure 10, it is possible that the pressure gradient at the leading edge on the upper surface prevents the flow from separating from the leading edge. At angles of attack above  $8^\circ$ , leading-edge separation is indicated by the ink-flow photographs which show outflow at the leading edge.

Wings With Semiapex Angles of  $22.5^\circ$

The vapor-screen photographs for the wings with semiapex angles of  $22.5^\circ$  (figs. 6 and 7) show separated regions at  $\alpha = 12^\circ$  for the wings with 10 and 20 percent of the semispans drooped. These separated regions are closer to the wing upper surface than the separated regions on the wings with a semiapex angle of  $15^\circ$ , but the spanwise location and extent of the separated regions are roughly the same for corresponding amounts of droop on the two sets of wings.

The pressure distributions shown in figures 12 and 13 show negative pressure peaks over the outboard portion of the wing upper surface for the

higher angles of attack with the primary effects of droop noted for the lower angles of attack and at the wing leading edge. The main difference between the pressure distributions of the wings with semiapex angles of  $15^\circ$  and  $22.5^\circ$  is that the spanwise decrease in pressure corresponding to the observed inboard extent of the region of separation is much more abrupt for the higher angles of attack on the wing with a semiapex angle of  $22.5^\circ$  than on the wing with a semiapex angle of  $15^\circ$ . The integrated pressure distributions in figure 17 show that, for equal angles of attack, the wing with 20 percent of the semispan drooped has considerably less loading than the wing with 10 percent of the semispan drooped.

Ink-flow test results obtained for the wing with 10 percent of the semispan drooped show a narrow line of ink (not to be confused with another narrow line at about the 94-percent-semispan position) at the very leading edge of the wing at  $\alpha = 12^\circ$ . (See fig. 20.) This indicates that the flow probably separates at the leading edge for this and higher angles of attack. As in the case of the wing with a semiapex angle of  $15^\circ$ , it is possible that the large pressure gradient at the leading edge for angles of attack of  $8^\circ$  and less prevents leading-edge separation at these angles.

#### Wings With Semiapex Angles of $31.75^\circ$

The vapor-screen photographs of the wings with a semiapex angle of  $31.75^\circ$  in figures 8 and 9 are different from those of the wings with semiapex angles of  $15^\circ$  and  $22.5^\circ$  in that shock waves are visible for the wings with 10 and 20 percent of the semispans drooped. These shock waves move inboard with increase in angle of attack, and regions of separation very close to the wing upper surfaces can be seen for the larger angles of attack.

The pressure distributions of figures 14 and 15 show abrupt spanwise decreases in pressure at positions corresponding to the observed inboard extent of the separated region and to the shock-wave locations for the higher angles of attack. Near the leading edges, the pressures show influences of leading-edge droop throughout the angle-of-attack range, especially on the wing with 20 percent of the semispan drooped. The ink-flow tests on the wing with 10 percent of the semispan drooped (fig. 21) indicate that there is probably no flow separation at the leading edges except possibly at  $\alpha = 20^\circ$ , although the pressure gradients at the leading edge for some of the lower angles of attack appear to be similar to that for  $\alpha = 20^\circ$ . The integrated pressure distributions of figure 18 indicate that, through the angle-of-attack range, there is slightly less loading on the wing with 20 percent of the semispan drooped than on the wing with 10 percent of the semispan drooped.

### Comparison With Flat-Plate Undrooped Wings

Some comparisons can be made of the results obtained in the present tests and the results presented in reference 1 for undrooped wings. As observed in the vapor-screen photographs, regions of separation first appear at higher angles of attack on the drooped wings than on the undrooped wings of reference 1, and, in general, the separated regions on the drooped wings are closer to the wing upper surface than those on the corresponding flat undrooped wings. For the drooped- and undrooped-leading-edge wings with semiapex angle of  $31.75^\circ$ , the positions of the shock waves are similar, but again the separated regions on the drooped wings are not as large as those on the undrooped wings.

The pressure distributions for the drooped and undrooped wings generally are similar for the higher angles of attack and at the inboard positions, but the effects of droop cause higher pressures at the outboard positions on the drooped wings. The integrated pressure distributions of figures 16 to 18 show that the drooped wings have less loading than the undrooped wings in all but one case, in which at the higher angles of attack drooped and undrooped wing loading are nearly equal, and these differences in loading are fairly large in some cases.

In general, the drooped-leading-edge wings show no particular advantage from a standpoint of preventing separation and, therefore, of possibly alleviating adverse vortex effects, since the separation phenomena for drooped and undrooped wings are similar. In the rather important consideration of loadings, the drooped wings have a disadvantage as compared with the undrooped wings, the loading in some cases being considerably less than that on the corresponding undrooped wing.

### CONCLUDING REMARKS

Vapor-screen, pressure-distribution, and ink-flow tests on delta wings with drooped leading edges and semiapex angles of  $15^\circ$ ,  $22.5^\circ$ , and  $31.75^\circ$  at a Mach number of 1.9 have shown that separated regions of vorticity existed along the upper surfaces of all the wings tested. In general, the separated regions on the wings with 10 percent and 20 percent of the semispans drooped were similar to one another. Integrated pressure distributions showed that, for equal angles of attack, the loadings on the wings with 20 percent of the semispans drooped were less than those on the wings with 10 percent of the semispans drooped.

In a general comparison with undrooped delta wings, the drooped-leading-edge wings showed no particular advantage from a standpoint of

preventing separation and thus of possibly alleviating adverse vortex effects. The drooped-leading-edge wings had a disadvantage in loading, the loading in some cases being considerably less than that on the corresponding undrooped wing.

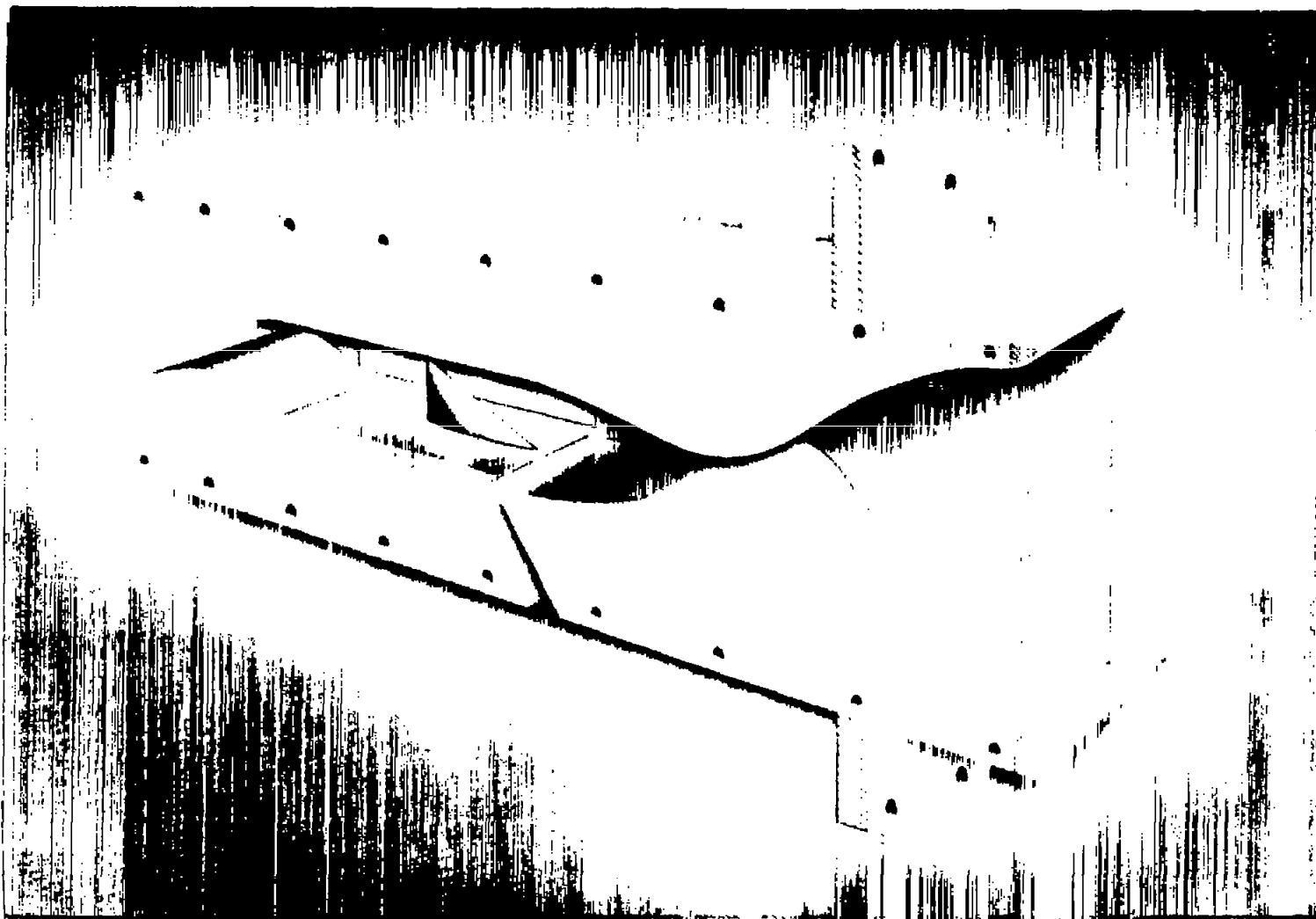
Langley Aeronautical Laboratory,

National Advisory Committee for Aeronautics,

Langley Field, Va., October 14, 1955.

#### REFERENCES

1. Michael, William H., Jr.: Flow Studies on Flat-Plate Delta Wings at Supersonic Speed. NACA TN 3472, 1955.
2. Allen, H. Julian, and Perkins, Edward W.: A Study of Effects of Viscosity on Flow over Slender Inclined Bodies of Revolution. NACA Rep. 1048, 1951. (Supersedes NACA TN 2044.)



L-80472

Figure 1.- View of blowdown jet showing the boundary-layer removal scoop.

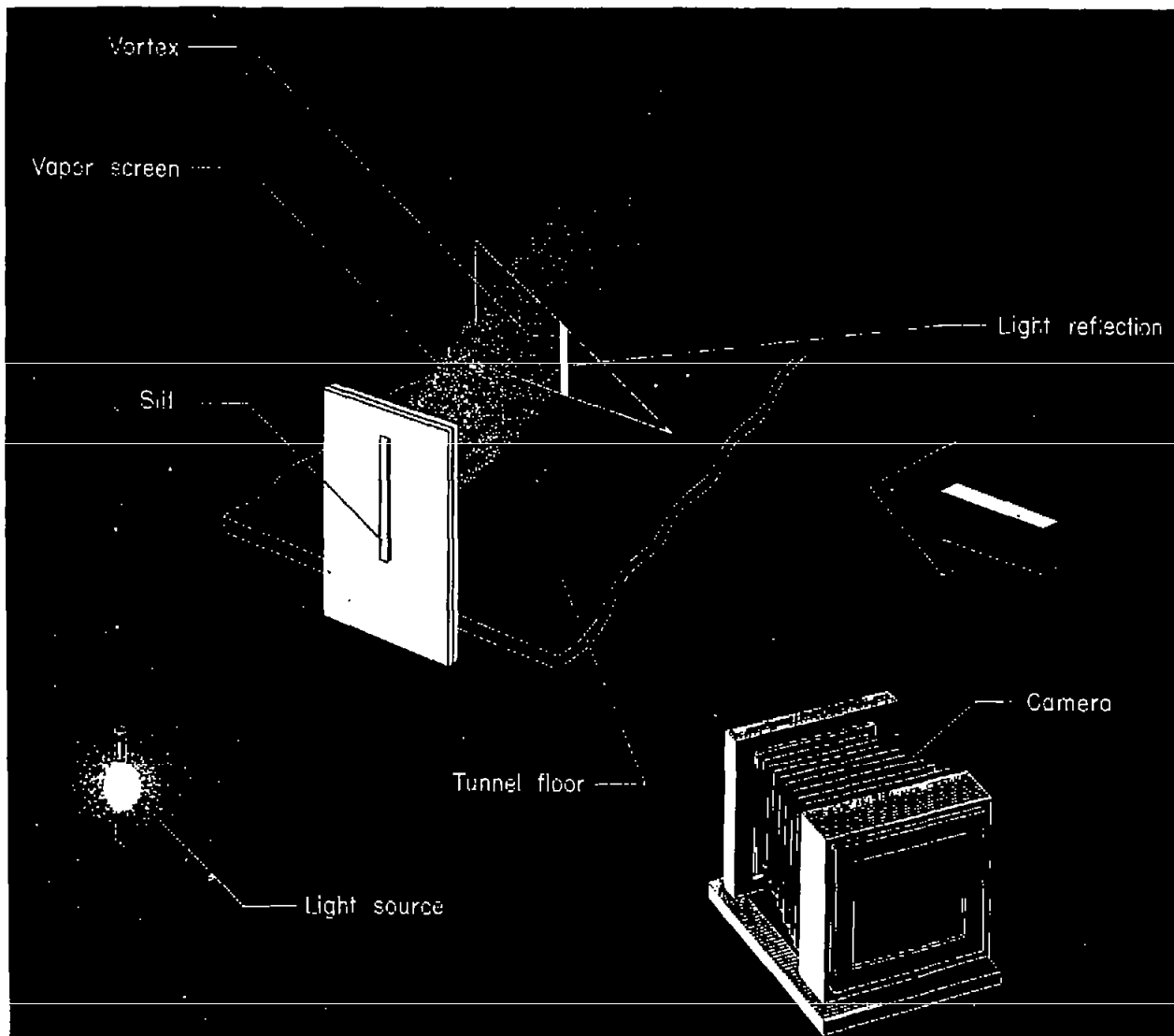


Figure 2.- Schematic drawing of vapor-screen apparatus and setup.

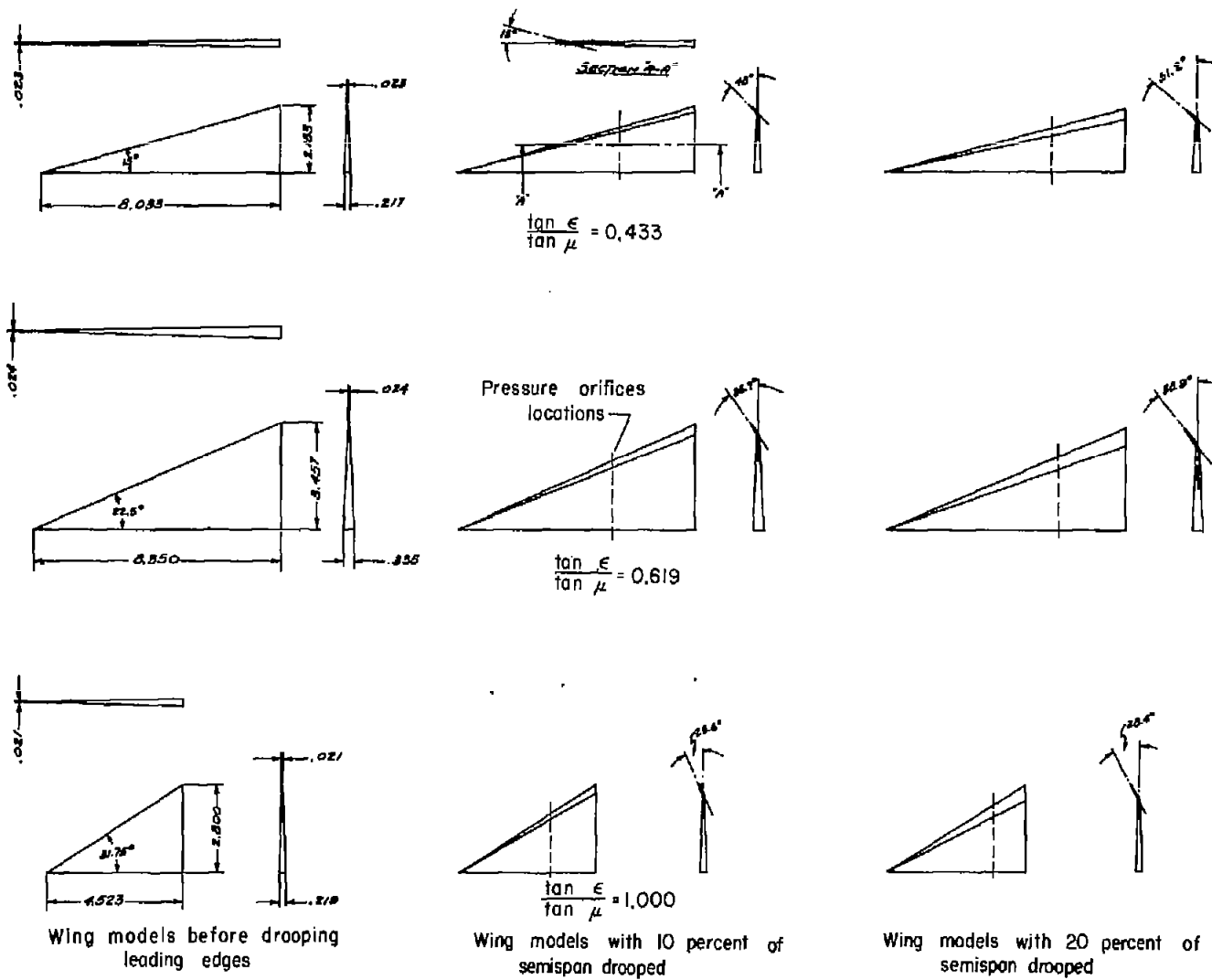


Figure 3.- Drawings of models. All dimensions are in inches.

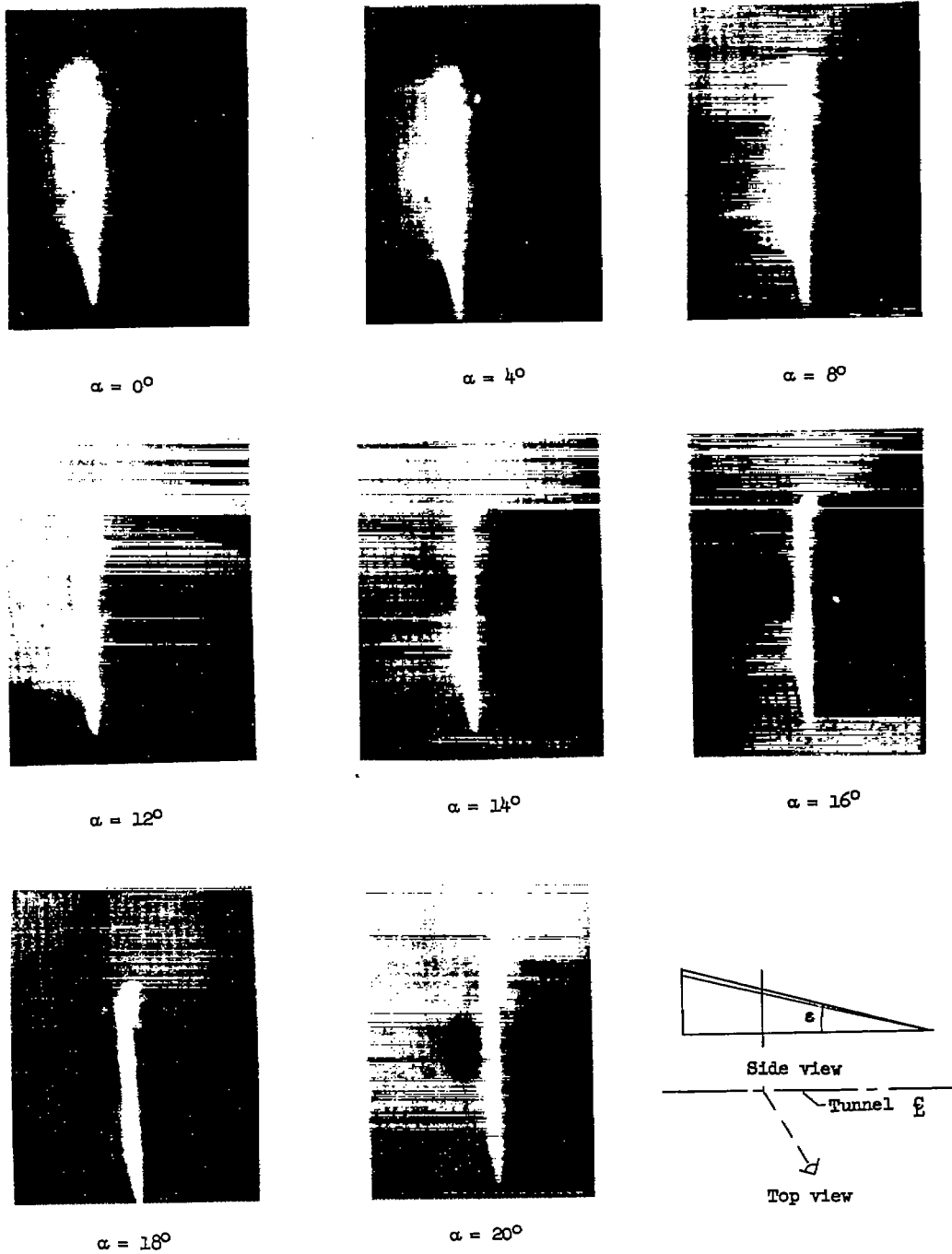
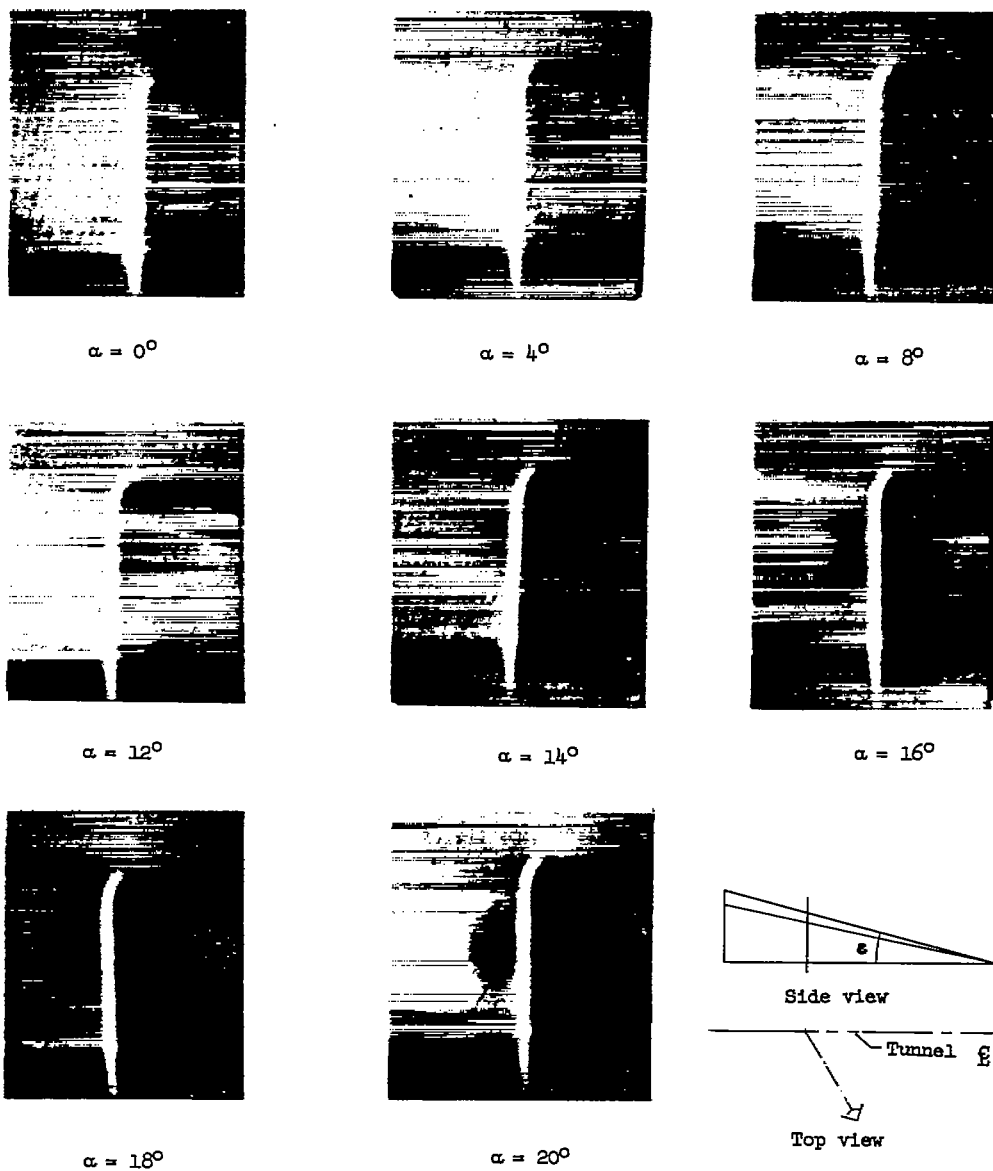


Figure 4.- Vapor-screen photographs of flow over wing with 10 percent of the semispan drooped.  $\epsilon = 15^\circ$ ; 68-percent-root-chord position.

L-90548



L-90549

Figure 5.- Vapor-screen photographs of flow over wing with 20 percent of the semispan drooped.  $\epsilon = 15^\circ$ ; 70-percent-root-chord position.

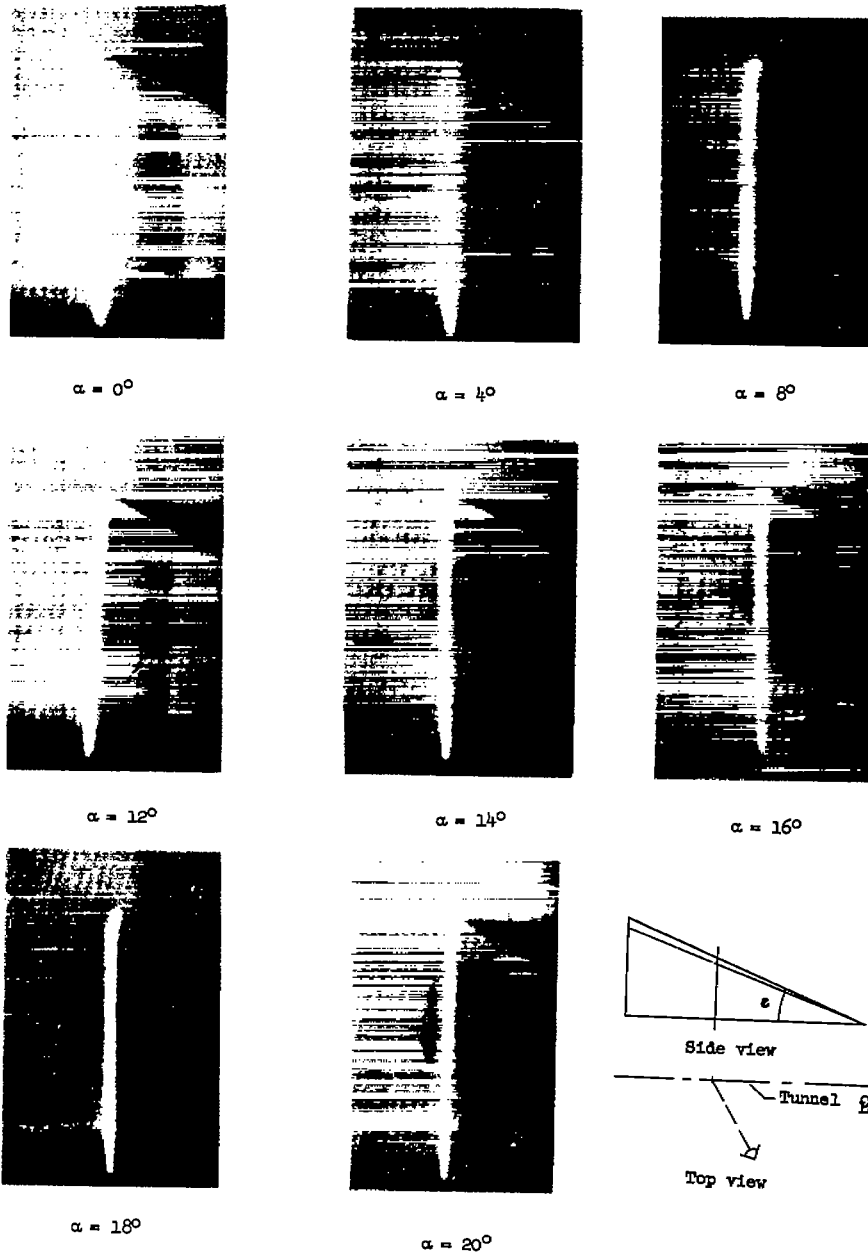
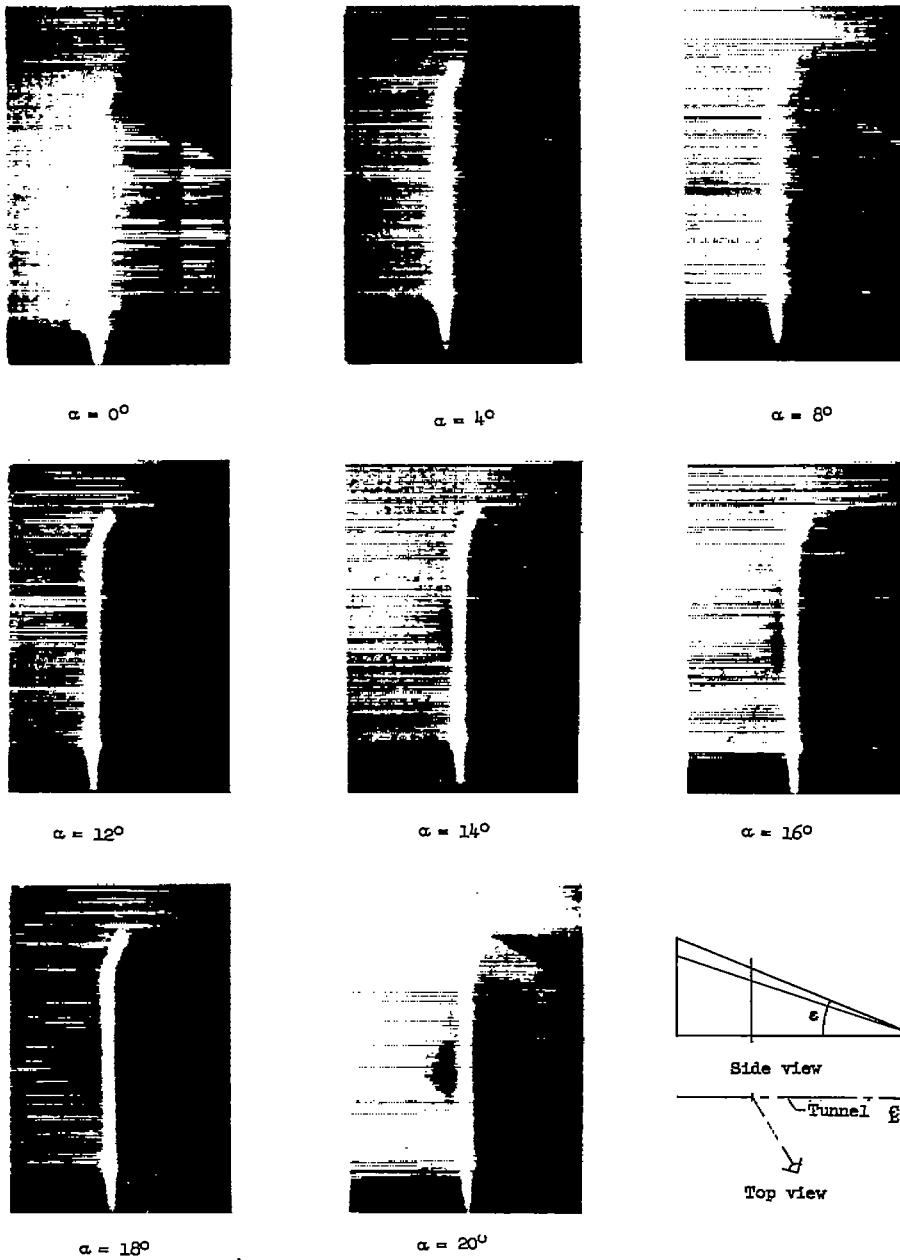


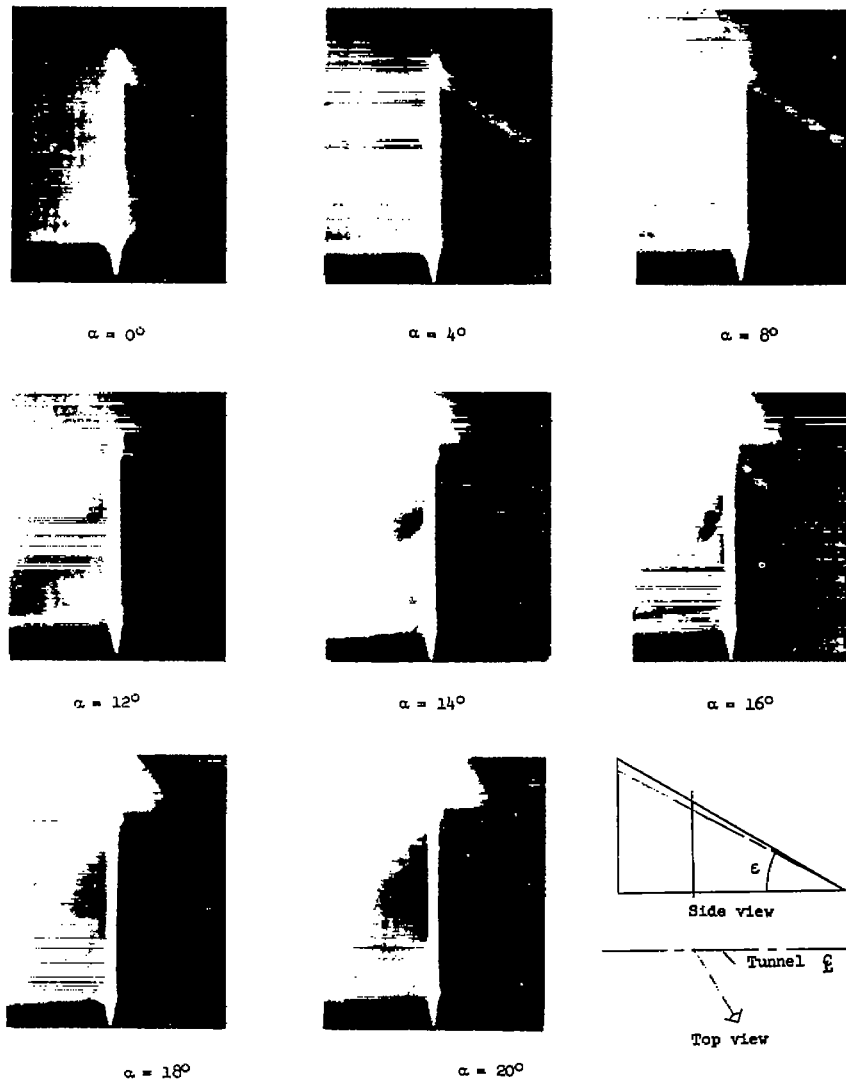
Figure 6.- Vapor-screen photographs of flow over wing with 10 percent of the semispan drooped.  $\epsilon = 22.5^\circ$ ; 62-percent-root-chord position.

L-90550



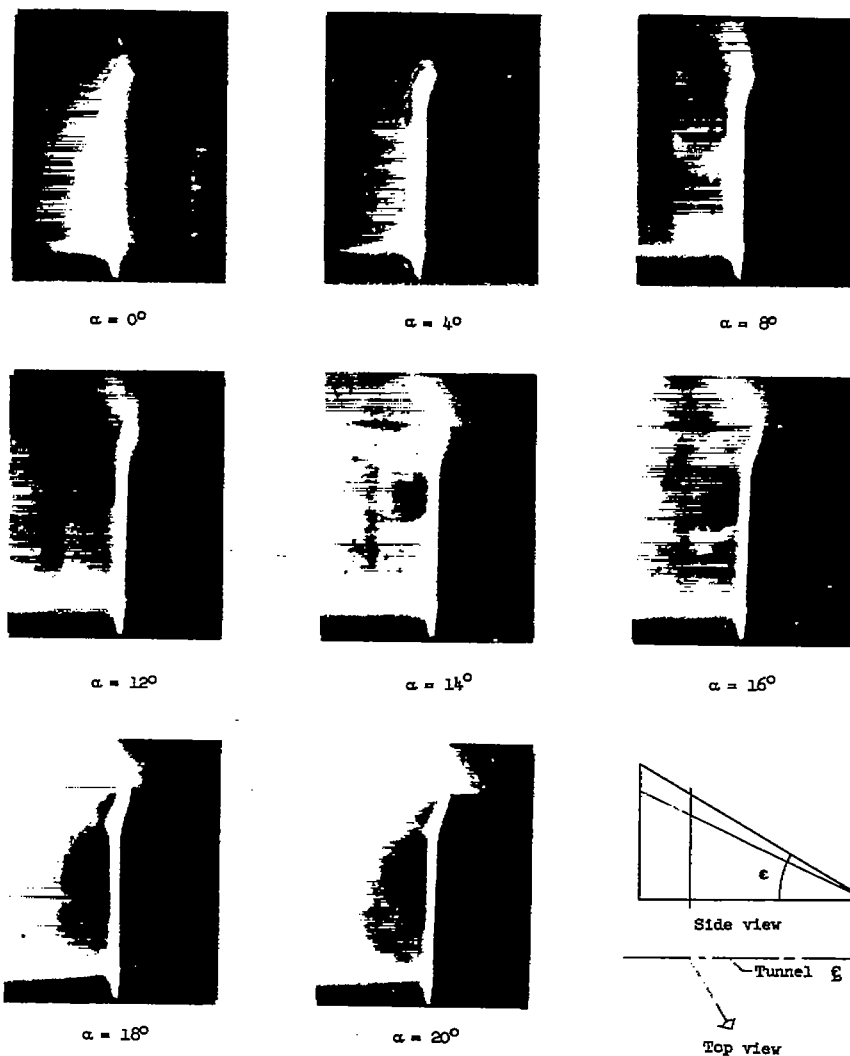
L-90551

Figure 7.- Vapor-screen photographs of flow over wing with 20 percent of the semispan drooped.  $\epsilon = 22.5^\circ$ ; 69-percent-root-chord position.



L-90552

Figure 8.- Vapor-screen photographs of flow over wing with 10 percent of the semispan drooped.  $\epsilon = 31.75^\circ$ ; 67-percent-root-chord position.



L-90553

Figure 9.- Vapor-screen photographs of flow over wing with 20 percent of the semispan drooped.  $\epsilon = 31.75^\circ$ ; 78-percent-root-chord position.

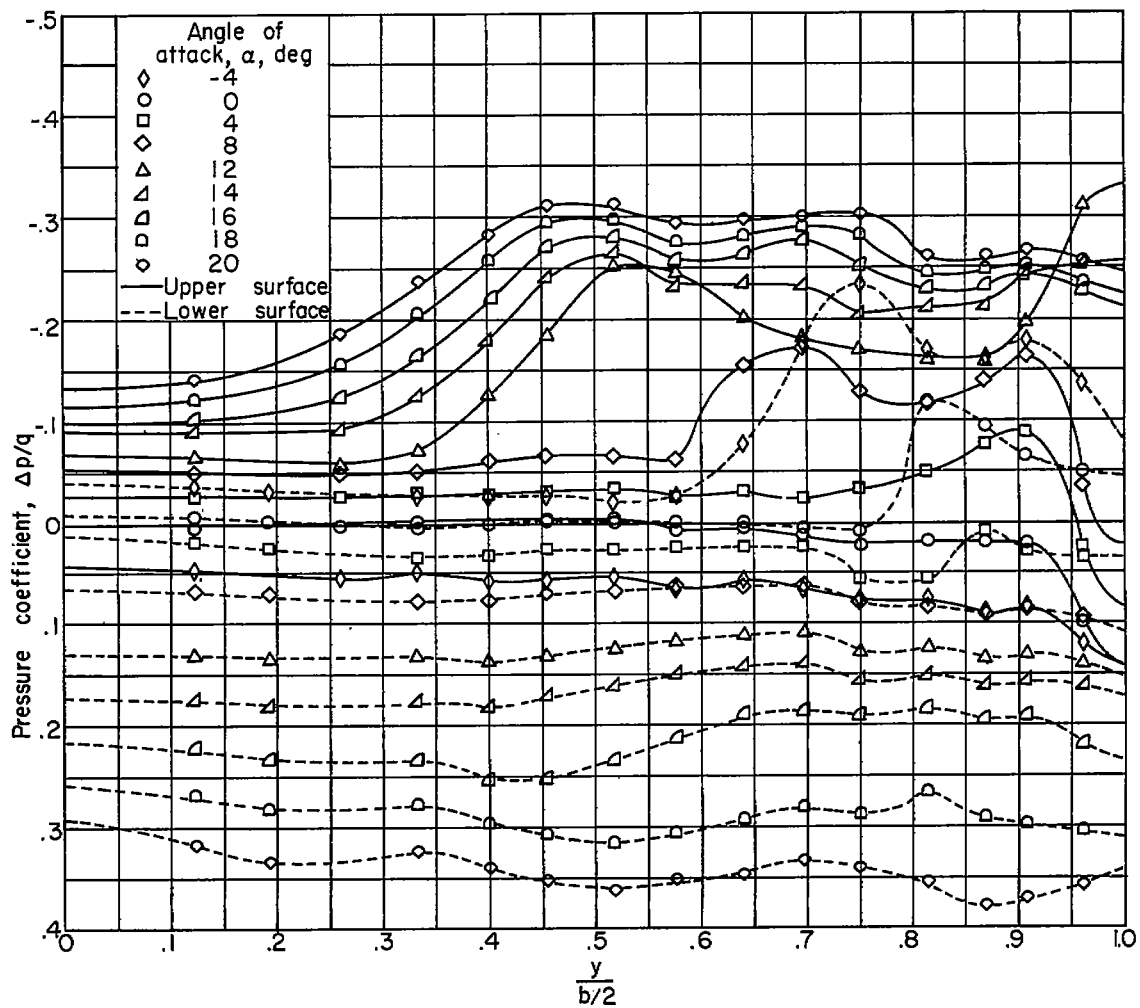


Figure 10.- Spanwise pressure distribution on wing with 10 percent of the semispan drooped.  $\epsilon = 15^\circ$ ; orifices located at 68.3-percent-root-chord position.

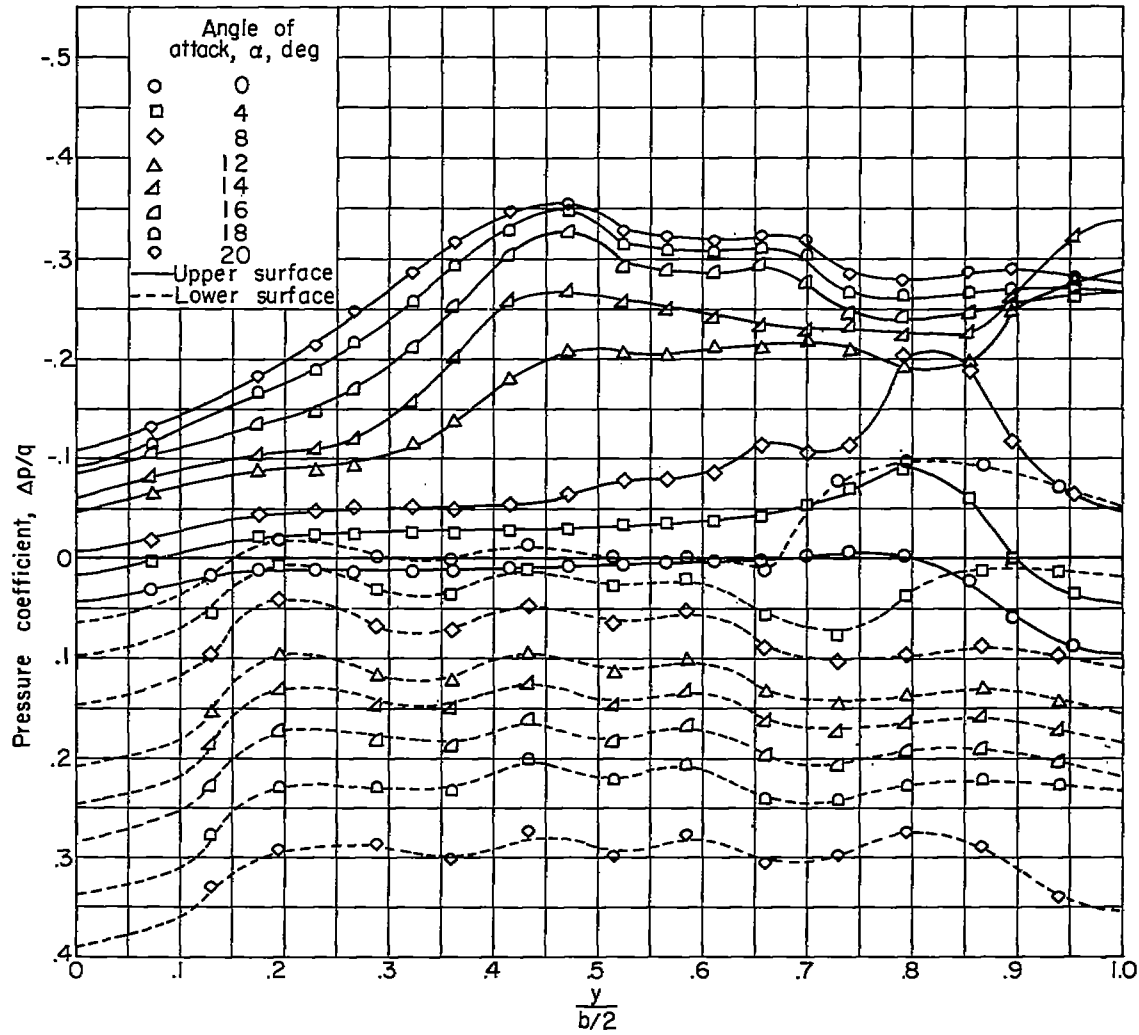


Figure 11.- Spanwise pressure distribution on wing with 20 percent of the semispan drooped.  $\epsilon = 15^\circ$ ; orifices located at 69.5-percent-root-chord position.

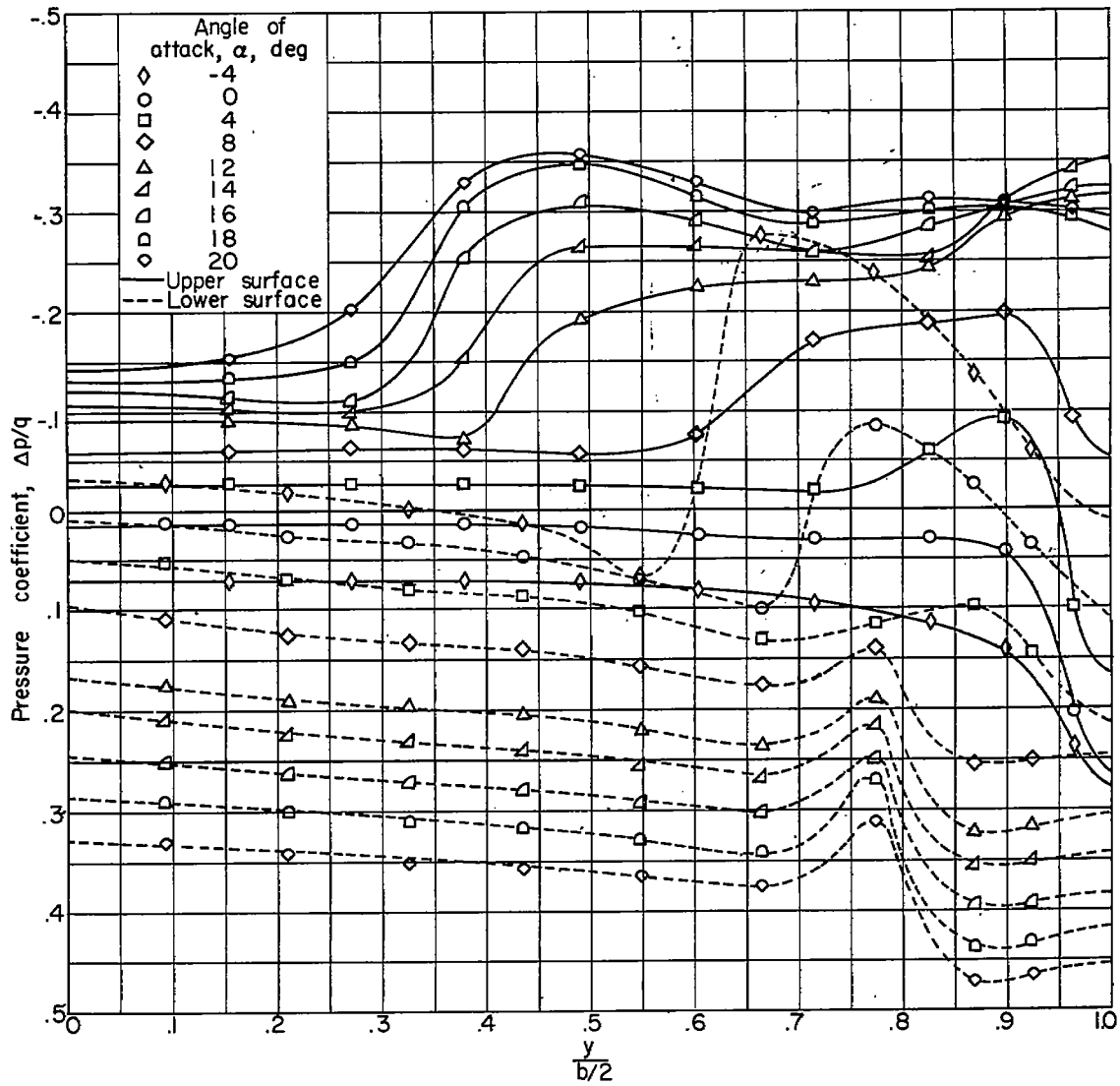


Figure 12.- Spanwise pressure distribution on wing with 10 percent of the semispan drooped.  $\epsilon = 22.5^\circ$ ; orifices located at 62.3-percent-root-chord position.

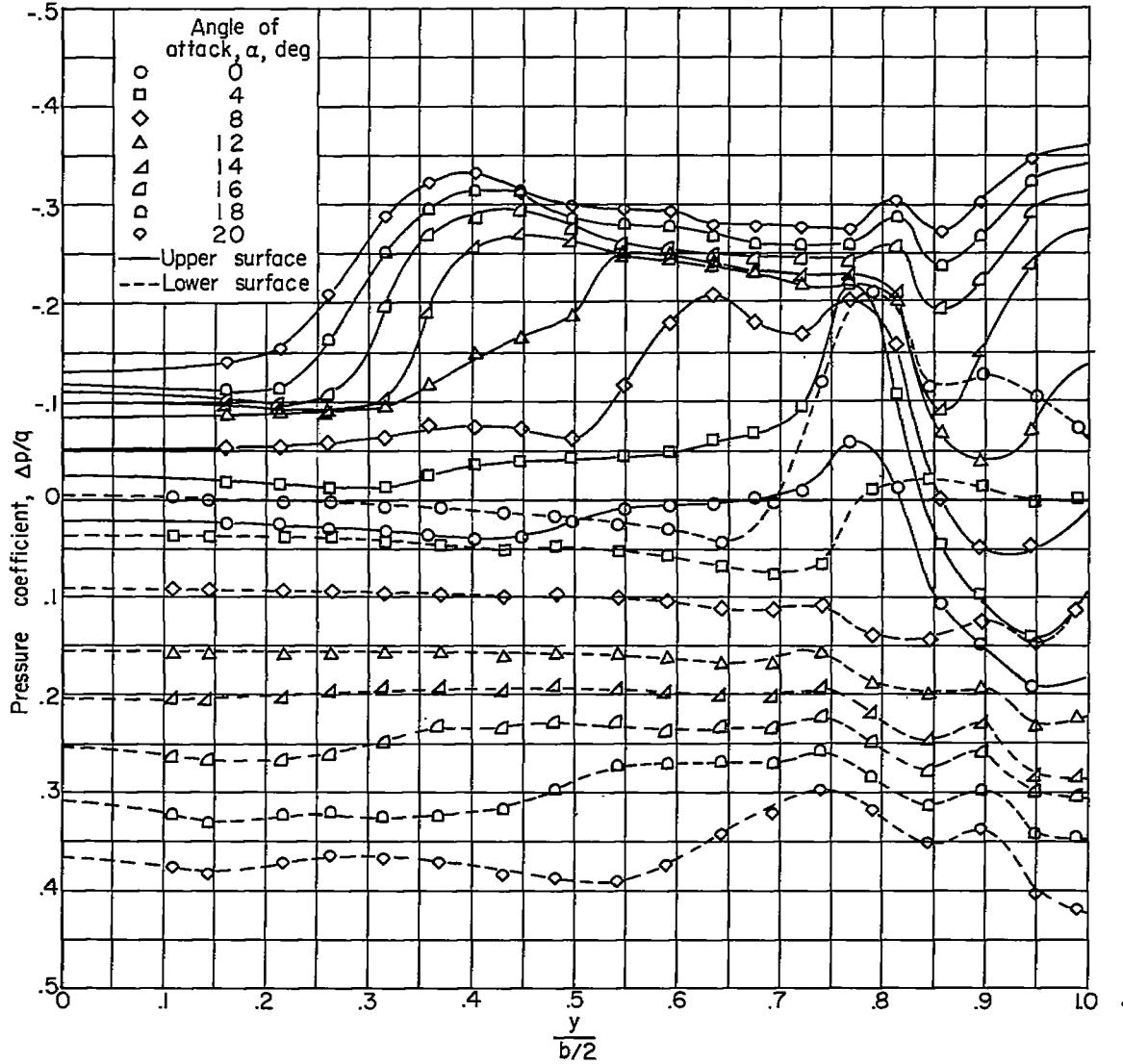


Figure 13.- Spanwise pressure distribution on wing with 20 percent of the semispan drooped.  $\epsilon = 22.5^\circ$ ; orifices located at 69.1-percent-root-chord position.

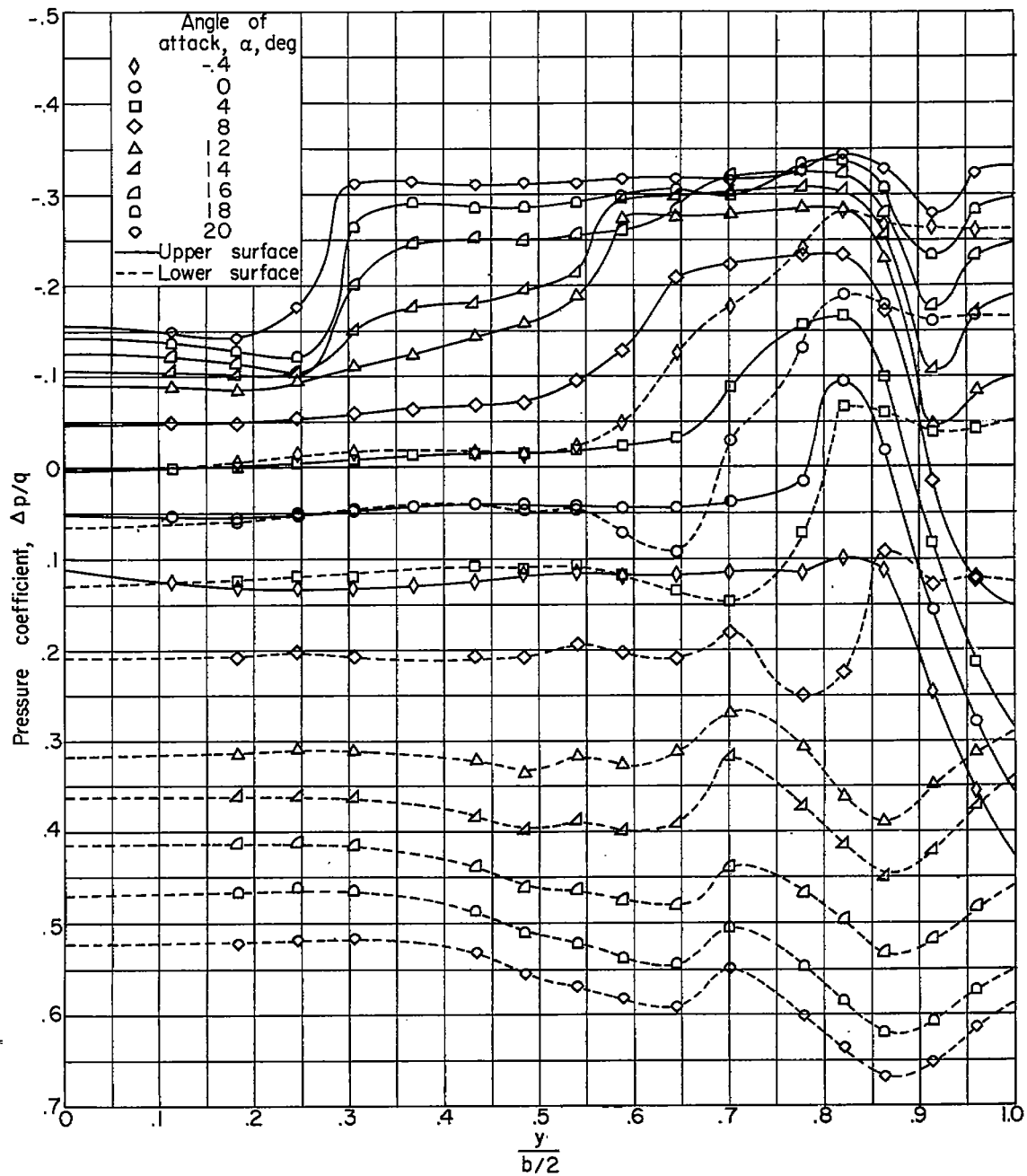


Figure 14.- Spanwise pressure distribution on wing with 10 percent of the semispan drooped.  $\epsilon = 31.75^\circ$ ; orifices located at 67.4-percent-root-chord position.

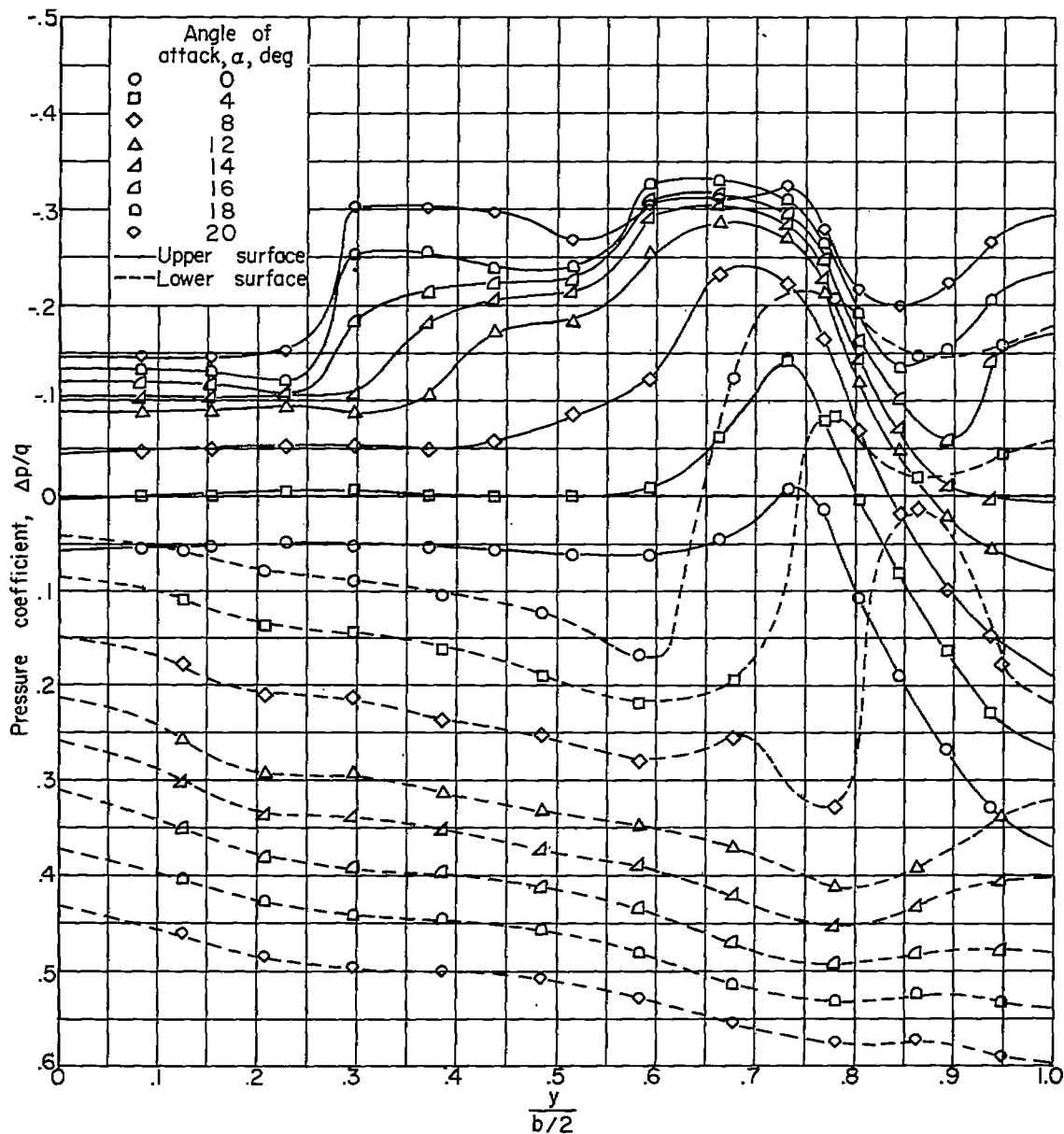


Figure 15.- Spanwise pressure distribution on wing with 20 percent of the semispan drooped.  $\epsilon = 31.75^\circ$ ; orifices located at 77.9-percent-root-chord position.

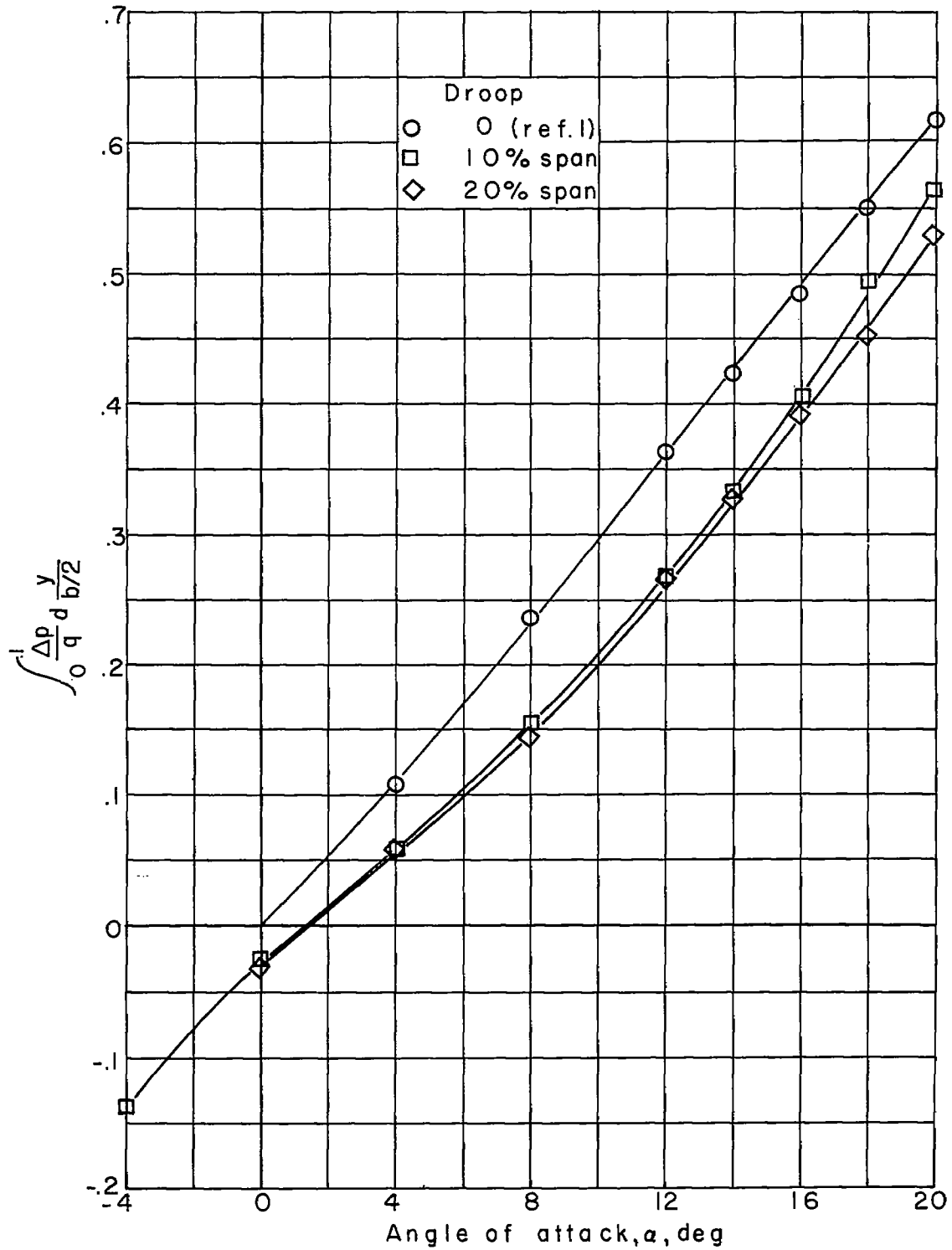


Figure 16.- Integrated pressure distributions for wing with  $\epsilon = 15^\circ$ .

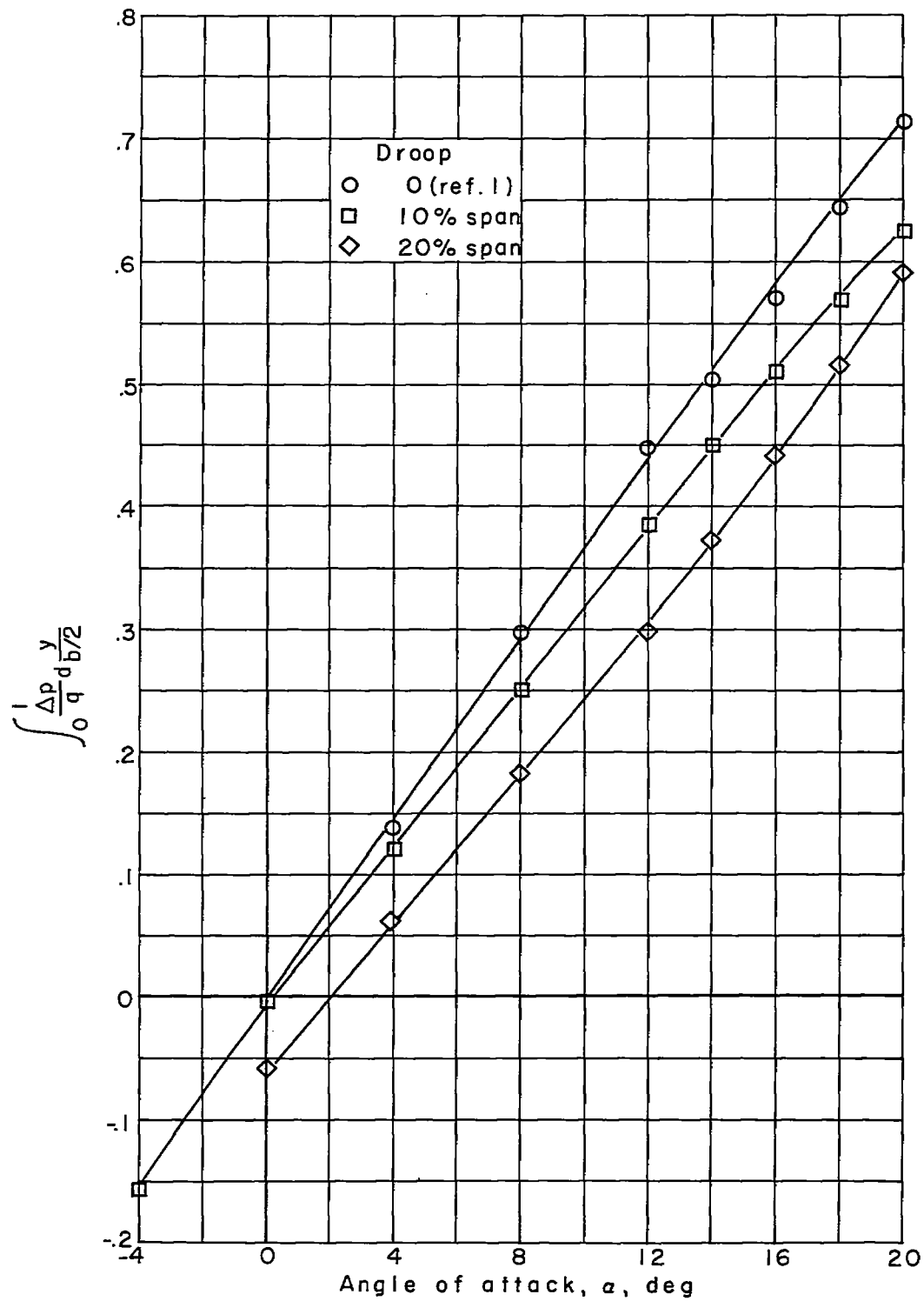


Figure 17.- Integrated pressure distributions for wing with  $\epsilon = 22.5^\circ$ .

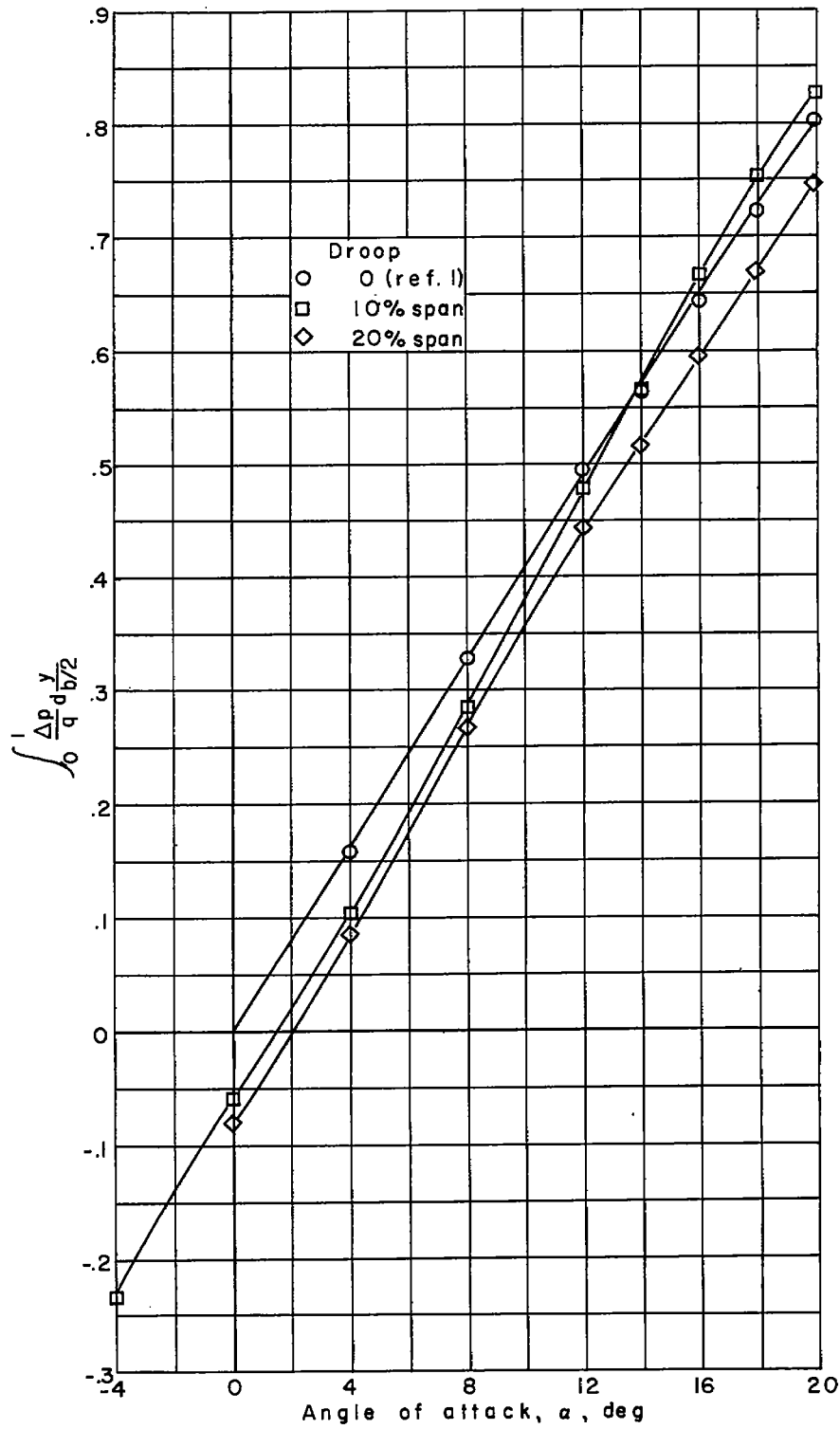


Figure 18.- Integrated pressure distributions for wing with  $\epsilon = 31.25^\circ$ .



$\alpha = -4^\circ$



$\alpha = 0^\circ$



$\alpha = 4^\circ$



$\alpha = 8^\circ$



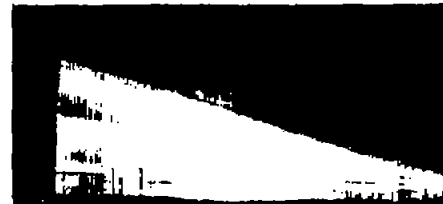
$\alpha = 12^\circ$



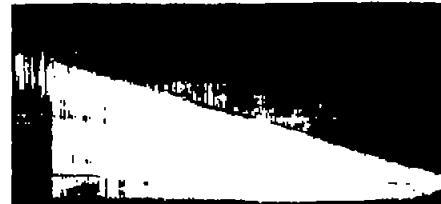
$\alpha = 14^\circ$



$\alpha = 16^\circ$



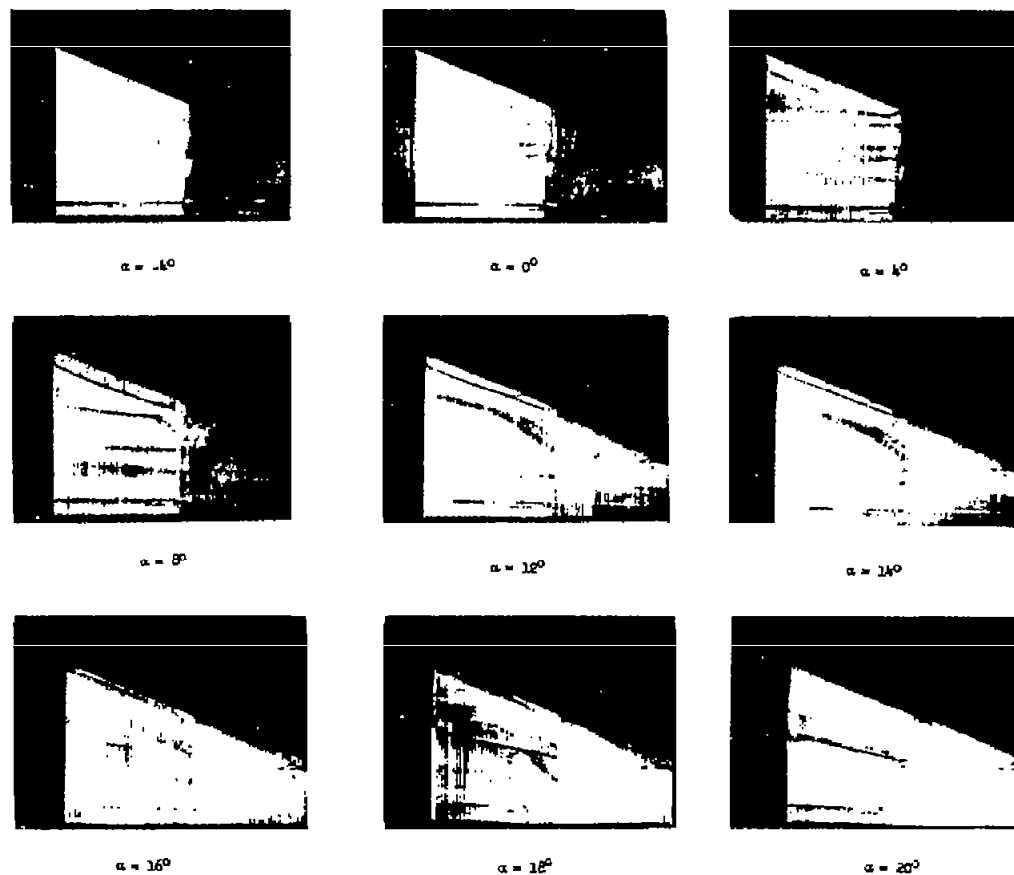
$\alpha = 18^\circ$



$\alpha = 20^\circ$

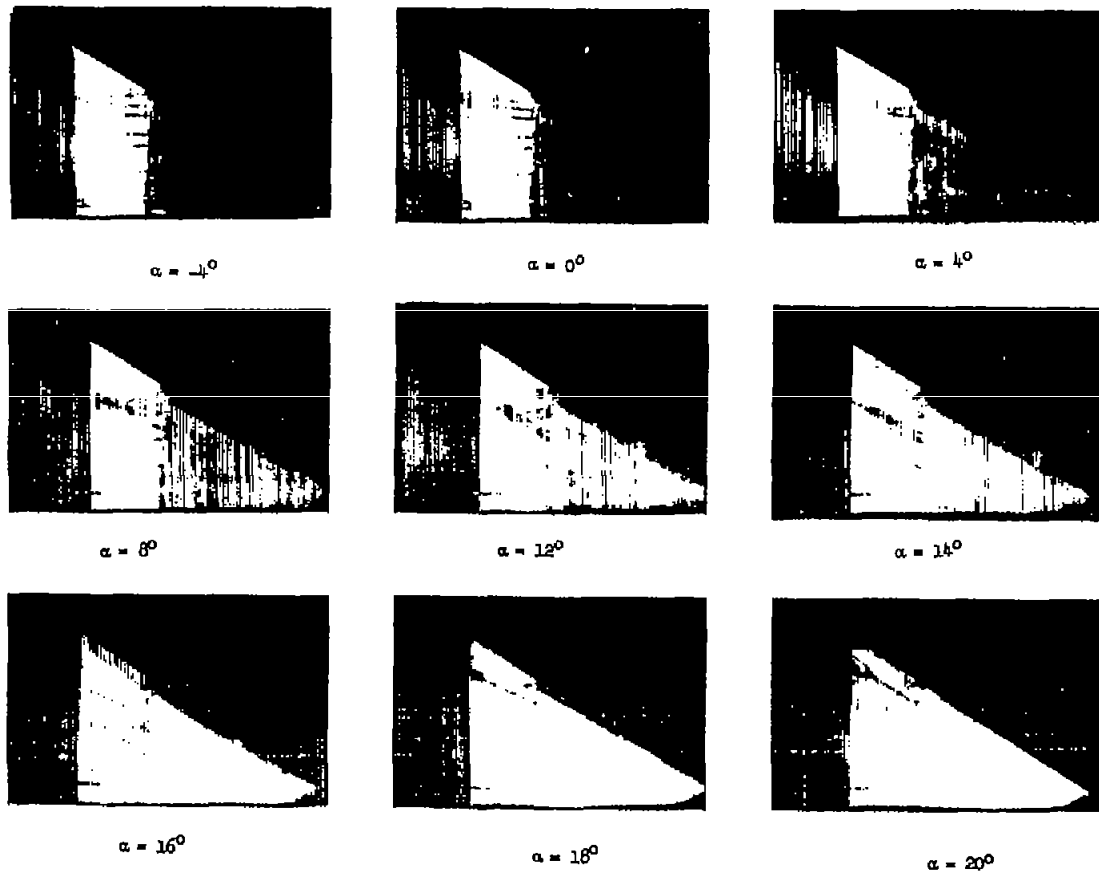
L-90554

Figure 19.- Ink-flow photographs for wing with 10 percent of the semispan drooped.  $\epsilon = 15^\circ$ .



L-90555

Figure 20.- Ink-flow photographs for wing with 10 percent of the semispan drooped.  $\epsilon = 22.5^\circ$ .



L-90556

Figure 21.- Ink-flow photographs for wing with 10 percent of the semispan drooped.  $\epsilon = 31.75^\circ$ .